

WALKING GAIT MEASUREMENT AND GAIT PARAMETERS
EXTRACTION

by
Chenye Li

A thesis submitted to the faculty of The University of Mississippi in partial fulfillment of
the requirements of the Sally McDonnell Barksdale Honors College.

Oxford
May 2018

Approved by

Advisor: Dr. Matthew Morrison

Reader: Dr. James Sabatier

Reader: Dr. Richard Gordon

© 2018
Chenye Li
ALL RIGHTS RESERVED

ACKNOWLEDGEMENTS

Foremost, I would like to thank the Sally McDonnell Barksdale Honors College and Department of Electrical Engineering for providing all the astonishing courses and massive resources that assist me with my work.

I would like to express my sincere gratitude to my thesis advisor Dr. Matthew Morrison. He offered me the summer internship opportunity doing research that demonstrated in this thesis. His guidance not only helped me writing the thesis, but also inspired me in multiple ways when I had a hard time doing my job. When I had questions, Dr. Morrison always responded immediately and fulfilled my needs.

I would also like to thank my supervisor Dr. James Sabatier the managing member of SOAIR LLC for supporting me doing the research and performing all the experiments. I thank my colleagues who worked on the same project with me and all the other SOAIR employees and former employees for providing help.

Last but not least, I would thank my family for respecting my choices on the academic carrier and giving me all the support. My accomplishment would not have been possible without them.

ABSTRACT

A fourth generation walking gait measurement device has been designed to capture and analyze detailed gait and stride metrics which eventually provides a Fall-Risk Assessment score. Specifically, the device has been modified to fit the residential environment and the elderly consumers which is low-cost, user-friendly, and portable. The gait parameters would be obtained by the on-board gait analysis protocol. Through gait parameters people's falling risk can then be calculated so that people can be alerted to take precautionary measures before falling. Overall, the device has been made and demonstrated having better performance than its previous generations. The on-board gait analyzing program executed slower than the computer version program but has the same accuracy. However, the overall performance is better than transforming data from the measurement device to a computer manually.

TABLE OF CONTENTS

ACKNOWLEDGEMENTS	iii
ABSTRACT	iv
LIST OF FIGURES	vii
LIST OF TABLES	viii
1. INTRODUCTION	1
1.1 BACKGROUND	1
1.2 PREVIOUS WORK AND ACHIEVEMENTS	2
1.3 CHALLENGES	4
2. DESIGN OF THE WALKING GAIT MEASUREMENT DEVICE	6
2.1 SYSTEM LAYOUT	6
2.2 MAIN OPERATION AND FUNCTION DESCRIPTION	6
2.2.1 OPERATION PRINCIPLE	6
2.2.2 ULTRASONIC SIGNAL TRANSMISSION AND RECEIVING	8
2.2.3 ANALOG TO DIGITAL (A/D) CONVERSION AND DEMODULATION	8
2.2.4 SIGNAL PROCESSING	9
2.2.5 OTHER FUNCTIONS	10
2.2.6 IMPROVEMENTS	10
2.3 PASSIVE INFRARED (PIR) SENSOR	12
2.4 ANALOG TO DIGITAL CONVERSION	14

3. GAIT ANALYSIS	15
3.1 STRIDE DATA EXTRATION	15
3.2 GAIT DATA CALCULATION AND APPROXIMATION	20
3.2.1 PEAK FOOT VELOCITY	21
3.2.2 STANCE TIME	21
3.2.3 SWING TIME	21
3.2.4 STRIDE TIME (GAIT CYCLE)	21
3.2.5 SWING/STANCE TIME	22
3.2.6 STANCE TIME PERCENTAGE	22
3.2.7 STEP CADENCE	22
3.2.8 STRIDE DISTANCE (STRIDE LENGTH)	23
3.2.9 AVERAGE STRIDE VELOCITY	23
3.2.10 DOUBLE STANCE TIME	23
3.2.11 SYMMETRY INDEX	24
3.2.12 GAIT SPEED	24
3.2.13 WALK RATIO	24
3.2.14 RESULTS EXAMPLE	25
4. CONCLUSION AND FUTURE DEVELOPMENT	26
4.1 CONCLUSION	26
4.2 FUTURE DEVELOPMENT	27
BIBLIOGRAPHY	28

LIST OF FIGURES

Figure 1.1 First Generation Prototype	2
Figure 1.2 Second Generation Porotype	3
Figure 1.3 Third Generation Prototype	4
Figure 2.1 System Layout (upper-left: raspberry pi3, upper-right: measurement computing 1608, lower-left: dc power supply, lower-right: analog board)	6
Figure 2.2 System Schematic	7
Figure 2.3 Fourth Generation Prototype Inside View (Left) and Outside View (Right)	11
Figure 2.4 PIR sensor (LHI986) and Fresnel Lens (EWA 0.4 GI V1)	12
Figure 2.5 Detection Range of LHI986 Constrained by Fresnel Lens	13
Figure 3.1 Original Walking Spectrogram from Decimated Demodulated Data	16
Figure 3.2 Wiener filtered Spectrogram in Gray Code	16
Figure 3.3 Foot Velocity	17
Figure 3.4 Smoothed Data with Peak Foot Velocity	17
Figure 3.5 Curve Fitted Foot Velocity	19
Figure 3.6 Ipsilateral (Red) and Contralateral (Black) Steps	20
Figure 3.7 Sample Result	25

LIST OF TABLES

Table 2.1 Comparison of 3 rd and 4 th Generation Device	11
---	----

1. INTRODUCTION

1.1 BACKGROUND

Gait parameter has been widely used in clinical injury diagnosis and treatment evaluation. Gait parameters are a reflection of multiple health status [1]. Specific parameters or data collection can be used to predict falls among patients [2] and elderly people [3]. Further studies have shown that proper gait measures may predict future risk of cognitive decline and dementia, which is preclinical marker for early treatment [2]. Therefore, daily gait measurement provides an important service for high risk populations, such as the elderly and recognized patients.

Visual observation while using a stopwatch is one of the most commonly used and simplest method to measure the gait velocity and stride time of the patient. However, more precise parameters, such as accurate electronic devices, are needed to predict the future risks. There are different approaches to achieve the measurement. A multiple camera system with electrodes on test subjects is the most reliable method to measure the gait [4]. However, it is hard to perform on a daily base without a well-trained person to use the system, and it is not affordable for normal family or individuals. Other approaches include single depth camera measure [5], radar measure [6-7], infrared measure [8], and ultrasonic measure [9]. In order to obtain the gait data, previous researchers used to obtain the body figures, or at least the body profile, with camera or infrared sensors to fit models and track

movements [10-11]. This thesis shows the method using ultrasonic transducers to measure human gait that do not recognize the outline of any body parts to keep privacy. In addition, the ultrasonic gait measuring is demonstrated to have a better accuracy compared to radar or infrared sensors [12].

1.2 PREVIOUS WORK AND ACHIEVEMENTS

Previously, three generations of ultrasonic gait measuring prototypes have been designed [13-14]. The first generation prototype was used to test the working principle where an ultrasonic transmitter and an ultrasonic receiver are drove by a laboratory function generator (HP 8904) and a data acquisition device (Wavebook 516E) shown in Figure 1.1. The data is saved and analyzed separately on a computer.

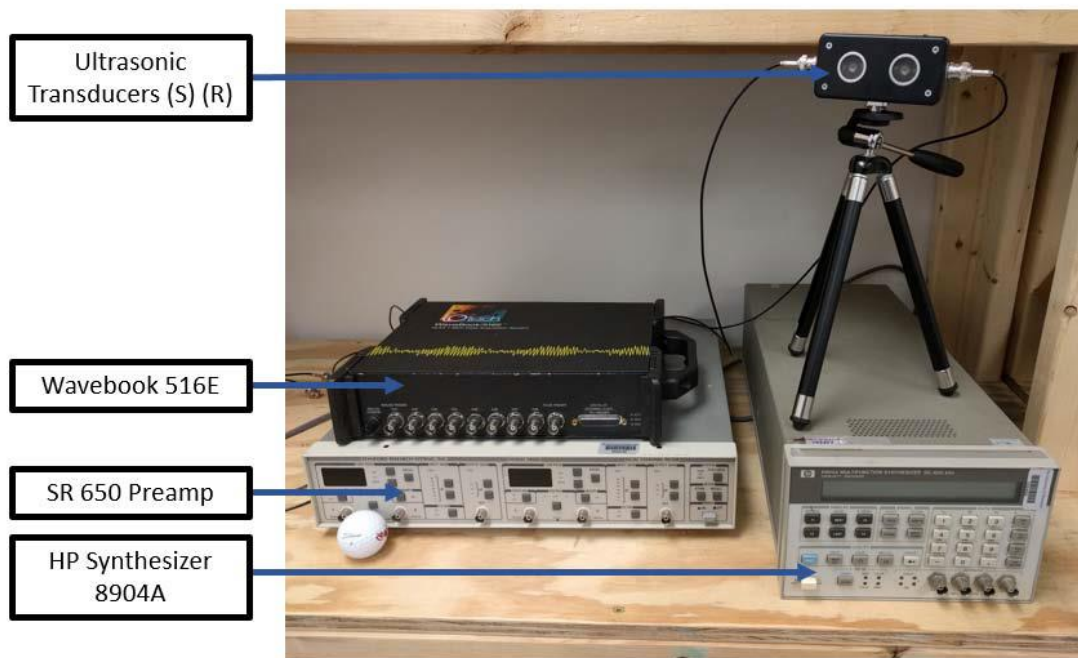


Figure 1.1 First Generation Prototype

The second generation prototype housed the preamplifier, ultrasonic transducers, and a data acquisition device (NI-USB 6216 DAC) in a box, which is portable for the field test. The box can directly connect to a computer that running a data analysis program. The inside and outside views of the box are shown in Figure 1.2.

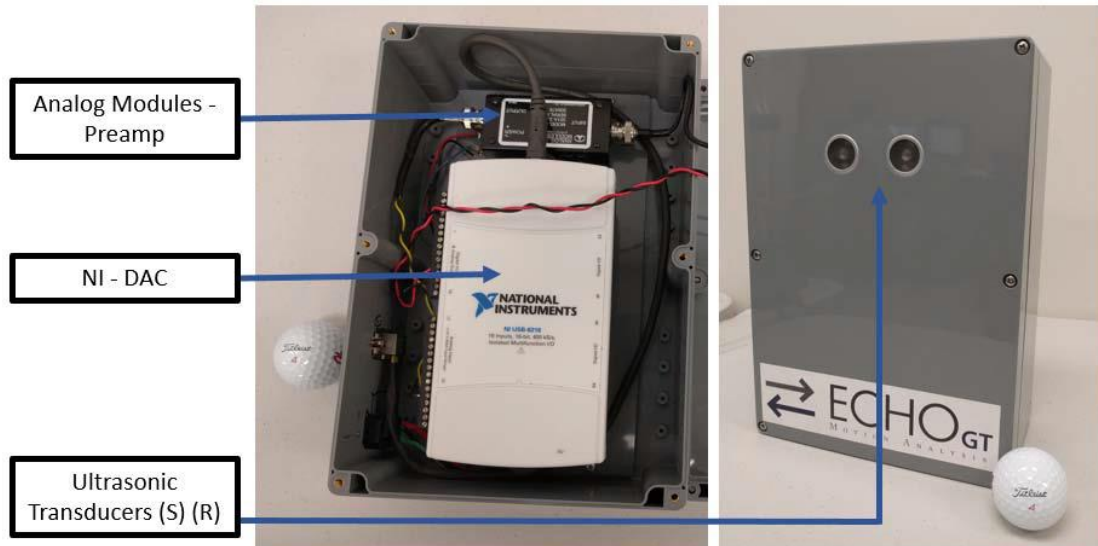


Figure 1.2 Second Generation Porotype

The third generation prototype added two functions to the second generation prototype. First, the device can be triggered automatically in PIR Mode. Second, it can be remote controlled by a separate raspberry pi with a touch screen. The box is redesigned with different components having same functions as the second one to achieve low cost. An additional computer is needed for data analysis. The inside and outside views of the box is shown in Figure 1.3.

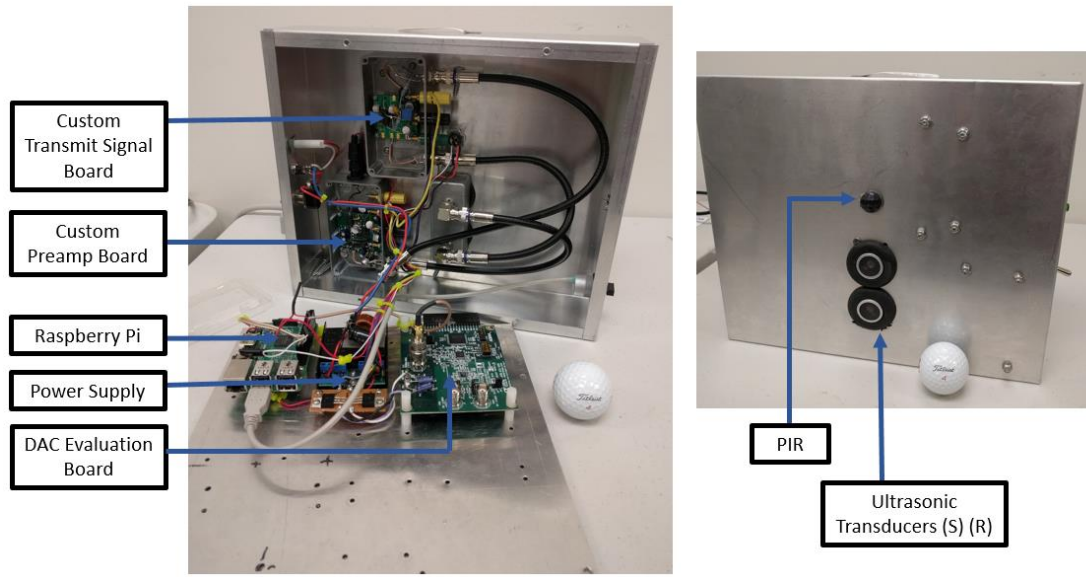


Figure 1.3 Third Generation Prototype

1.3 CHALLENGES

Based on the previous work, a newly designed device addresses all the issues occurring in the third generation prototype as following.

- 1) Program settings does not match the hardware settings.

The analyzing program (or image processing program) is written for data that is sampled at 100 kHz, however, the analog to digital conversion system (LTI Board) can only sample data at 96 kHz limited by industry standard that used.

- 2) PIR sensor has probably misrecognize motion.

The PIR sensor can detect very wide range movement. However, good data can only be obtained with straight walk toward or away from the ultrasonic transmitter and receiver. Thus, unwanted data is taken when subjects are at bad position or simply walk across the detection area.

3) No on-board data analysis.

A separate computer is needed for off-board data and image processing.

2. DESIGN OF THE WALKING GAIT MEASUREMENT DEVICE

2.1 SYSTEM LAYOUT

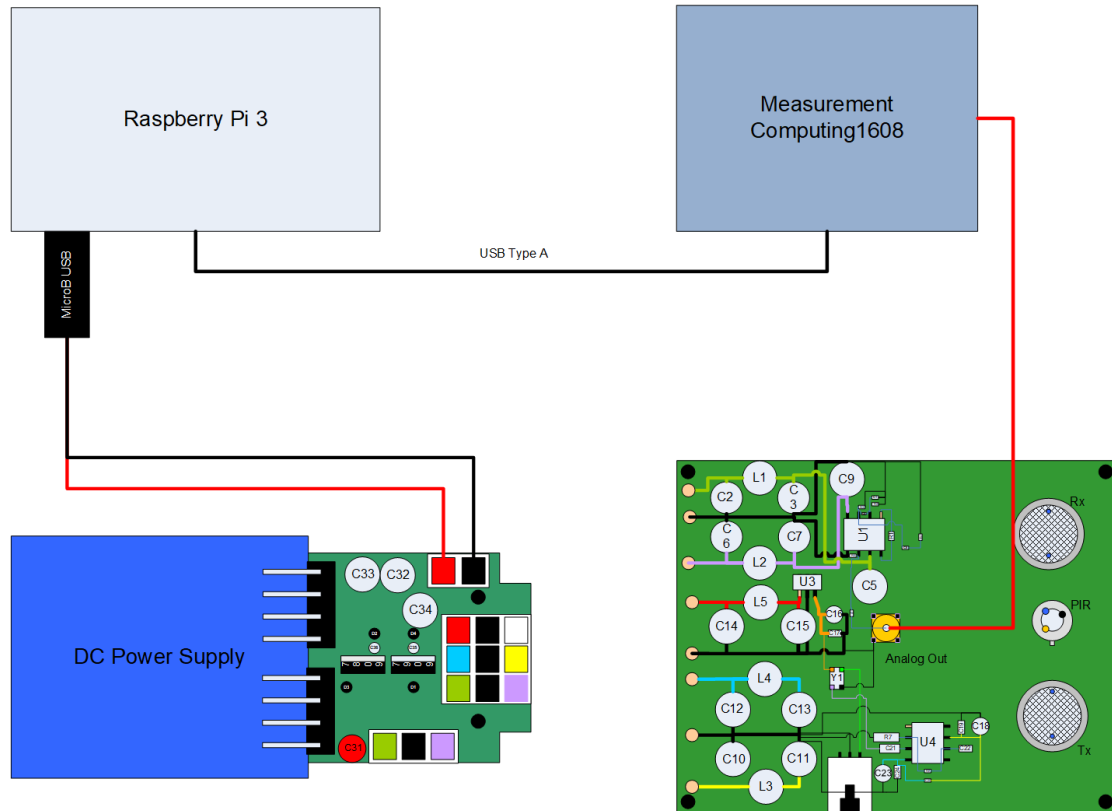


Figure 2.1 System Layout (upper-left: raspberry pi3, upper-right: measurement computing 1608, lower-left: dc power supply, lower-right: analog board)

2.2 MAIN OPERATION AND FUNCTION DESCRIPTION

2.2.1 Operation Principle

The principle of the 4th generation ultrasonic walking gait measurement device is based on the Doppler shift in frequency of a moving object, where the frequency shift is

directly proportional to the vibration velocity of the target [15]. The schematic of the device is shown in Figure 2.2.

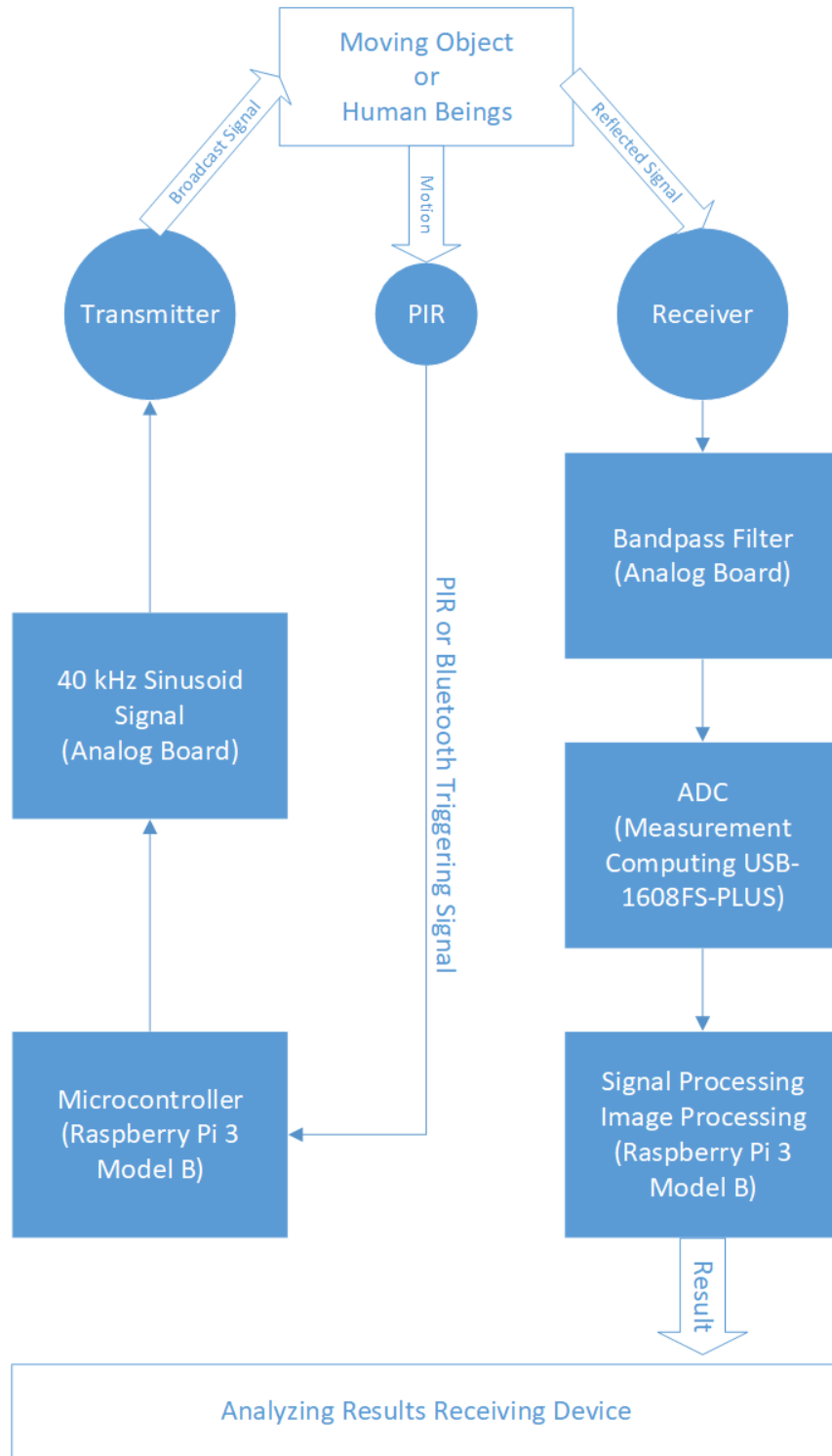


Figure 2.2 System Schematic

2.2.2 Ultrasonic Signal Transmission and Receiving

As shown in the Figure 2.1, the device operated with two ultrasonic transducers, one as a transmitter and the other as a receiver. The transmitter broadcasts a 40 kHz sinusoid signal generated by the Analog Board. The receiver turns on at the same time to obtain signal from the vibrating surface which is a result of the Doppler Effect [16]. With the moving objects, a phase shift in the signal occurs which is used to detect the movement.

Expressed as:

$$g(t) = A \cos(2\pi f_c t + \varphi(t)),$$

$$\varphi(t) = \frac{4\pi}{\lambda} \int_{-\infty}^t v(\tau) d\tau + \varphi_0,$$

$$v(t) = f_d(t) \frac{v_{sound}}{2f_c},$$

where f_c is the carrier frequency, v is the speed of the moving target, f_d is the Doppler frequency.

2.2.3 Analog to Digital (A/D) Conversion and Demodulation

The A/D conversion and demodulation are performed on the Measurement Computing 1608 (MC1608). The A/D conversion comes after a wide band-pass filter to prevent data loss and distortion. After conversion, the received signal is multiplied by the carrier signal and its $\pi/2$ shifted version expressed as:

$$g(t) \times g_c = \frac{1}{2} [\cos(4\pi f_c t + \varphi) + \cos(\varphi)],$$

$$g(t) \times g_{co} = \frac{1}{2} [\sin(4\pi f_c t + \varphi) + \sin(\varphi)],$$

where

$$g_c = B \cos(2\pi f_c t),$$

$$g_{co} = B \cos\left(2\pi f_c t - \frac{\pi}{2}\right) = B \sin(2\pi f_c t).$$

The in-phase component $I(t)$ and quadrature component $Q(t)$ and be extracted after low pass filtering [17]. The Doppler signal can then be expressed as follow:

$$S(t) = I(t) + jQ(t),$$

where

$$I(t) = \cos(\varphi),$$

$$Q(t) = \sin(\varphi).$$

2.2.4 Signal Processing

As long as the raspberry pi 3 receives the demodulated data, an on-board image processing program extracts the gait parameters of which the detail will be discussed in Section 3.

Previously, to analyze data, program relied on MATLAB Runtime library has been written and run on computer. However, MATLAB does not have a raspberry pi version library or library that is written for ARM based CPU. Therefore, GNU Octave has been used to replace the MATLAB to run its code. The syntax of GNU Octave is similar to MATLAB, but the libraries and functions have a huge difference. Due to the missing of some very important signal processing functions, several functions have been rewritten and optimized in GNU Octave syntax. As a result, it takes around 80 seconds to finish

running the whole GNU Octave processing program on raspberry pi 3 compared to around 15 seconds for the MATLAB program running on 3.2 GHz quad-core computer.

2.2.5 Other Functions

The device can be either triggered automatically by a passive infrared (PIR) sensor (on PIR Mode) or triggered manually by another raspberry pi with touch screen (on Bluetooth Mode). After being triggered the device will take data for ten seconds and temporarily store in the in-box raspberry pi. Since the gait information can be obtained by the on-board programs, it can be upload onto the online database or send to any personal devices that connected.

2.2.6 Improvements

Compared to the 3rd generation, the 4th generation walking gait measurement device improves its performance in multiple aspects. First, the redesigned hardware layout reduces the length of wiring and communication times between difference PCBs and microcontrollers. Second, the improvement of the PIR sensor reduces data redundancies and data verification which will be discussed in Section 2.3. Third, on-board data analysis is achieved on 4th generation device. Figure 2.3 shows the design of the 4th generation device. Table 2.1 list the included hardware in both 3rd and 4th generations.

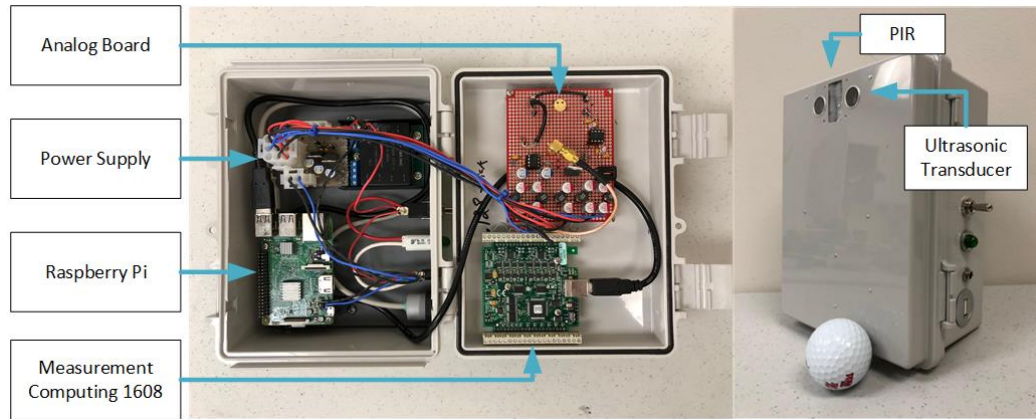


Figure 2.3 Fourth Generation Prototype Inside View (Left) and Outside View (Right)

3rd Generation	4th Generation
Raspberry Pi 2	Raspberry Pi 3
Linear Technology Board	Measurement Computing Board
Crystal Oscillator	Analog Board
Preamplifier	
Ultrasonic Transmitter & Receiver	Ultrasonic Transmitter & Receiver
PIR Sensor	PIR Sensor and Fresnel Lens
Power Supply	Power Supply
Raspberry Pi with a Touch Screen (Bluetooth)	Personal Electronic Device (not Included)
Computer	

Table 2.1 Comparison of 3rd and 4th Generation Device

2.3 PASSIVE INFRARED (PIR) SENSOR

The PIR sensor in the 3rd generation device has a wider detection range than the ultrasonic transducer. This means that the device will be falsely triggered even the target is out of the effective range of detection. The solution is to use a Fresnel lens to narrow down the detection range of the PIR sensor.

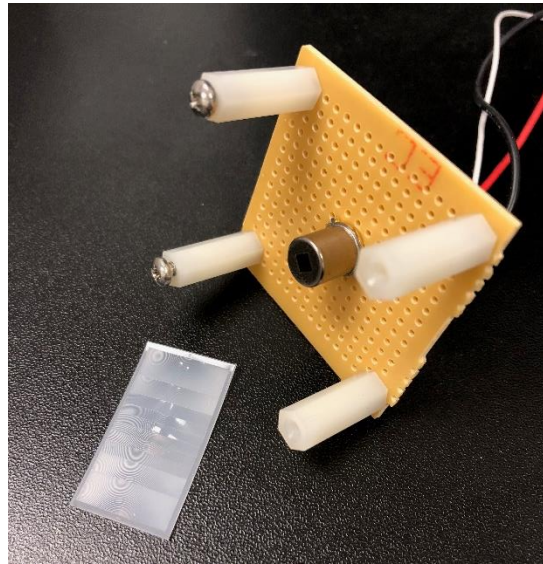
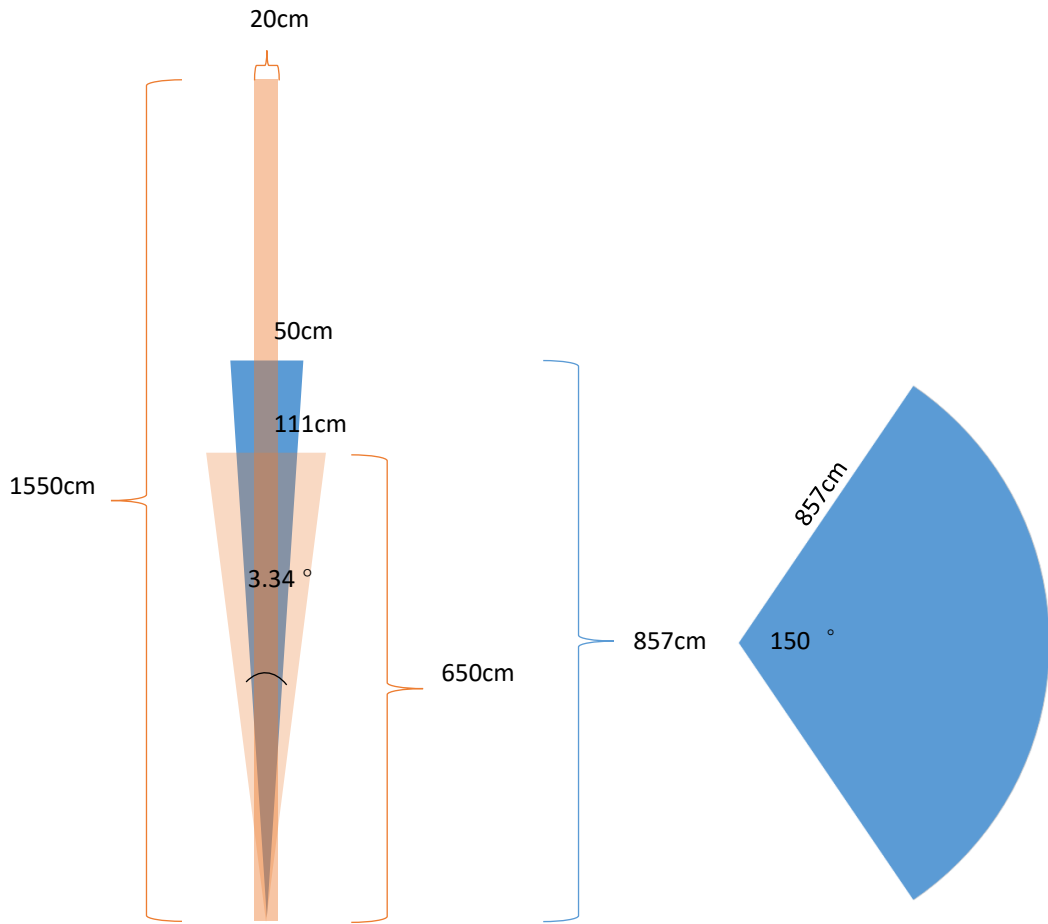


Figure 2.4 PIR sensor (LHI986) and Fresnel Lens (EWA 0.4 GI V1)

Converged by the customized Fresnel lens EWA 0.4 GI V1 the analog version PIR sensor LHI986 comes out a narrow detection width on one side and a wide range when rotates 90 degrees. The sensor and lens are placed aligned and vertical to the ground so that it can only detect motions right in front of it. In addition, as the detection range of the other side is wide, the motion of people with different heights can be easily detected.



Top View of the Beam

Side View of the Beam

- Effective area that can detect motion of walking across the beam.
- Effective area that can detect motion of walking toward and away from the sensor.

Figure 2.5 Detection Range of LHI986 Constrained by Fresnel Lens

2.4 ANALOG TO DIGITAL CONVERSION

In the 3rd generation device the ADC (LTI Board) was built using I2S protocol which can only work on the multiples of 24 kHz, such as 96 and 192 kHz. This does not match the existing image processing algorithm that set at 100 kHz sampling rate.

Considering that the benchmark of the algorithm has been set and tested throughout the previous generations of the device, the first attempt is to work out another ADC solution the match the preferred parameter.

Measurement Computing USB-1608FS-PLUS (MCC) has 16 channels which allowing digital I/O and analog I/O. 2 channels has been used as analog to digital converter. To program the device a C library for Linux based system written by Warren J. Jasper has been applied.

3. GAIT ANALYSIS

3.1 STRIDE DATA EXTRACTION

As long as the data has been collected from the analog board and converted to digital signal with the Measurement Computing A/D Converter, it will then process by the Raspberry Pi 3 where the stride data will be extracted and calculated. Virtually, a spectrogram is plotted with the demodulated data sets. It can be expressed as a square of the short-time Fourier transform (STFT).

$$STFT(t, f) = \int S(t + \tau)w(\tau) \exp(-j2\pi f\tau) d\tau$$

The following procedures aim to find the stride data based on the spectrogram.

Figure 3.1 is a spectrogram of time versus walking velocity. The total sample time is 10 second. It is shown that the subject in the experiment walks toward to the transducers from a distance, as the strength of the signal become higher when close to the end. In addition, the magnitude of the signal increases approximately from 0 to 1 second, and it decreases at the last second. This indicates that the subject started walking and speeded up for about 1 second, kept a constant speed for about 8 second, and slowed down at the end. Each ripple in the figure represent a step or a swing of one foot, and any two ripples next to each other are steps of left and right foot respectively. Only strides in the constant speed portion is considered as effective strides for the gait parameter calculation. Therefore, the objective of this procedure is to extract and analysis strides at the constant speed portion.

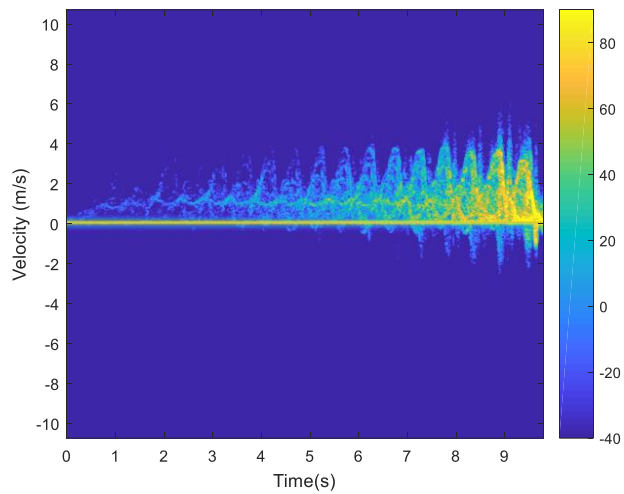


Figure 3.1 Original Walking Spectrogram from Decimated Demodulated Data

To extract the stride pattern, the spectrogram is first turned in to gray code where a threshold is set, as a result enhancing the contrast. The part with negative velocities which considered as noise is cut. Then, a Wiener filter is applied to minimize the mean square error between the estimated random process and the desired process, in other word, to reduce the Gaussian noise [18]. The result is shown in Figure 3.2.

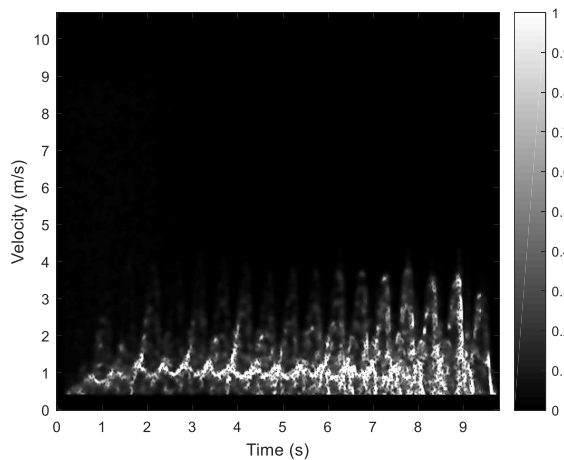


Figure 3.2 Wiener filtered Spectrogram in Gray Code

To calculate gait parameters, foot velocity is needed. While walking, toe and heel have the maximum velocity which is represented by the envelope of the spectrogram.

Figure 3.3 shows the envelope extracted.

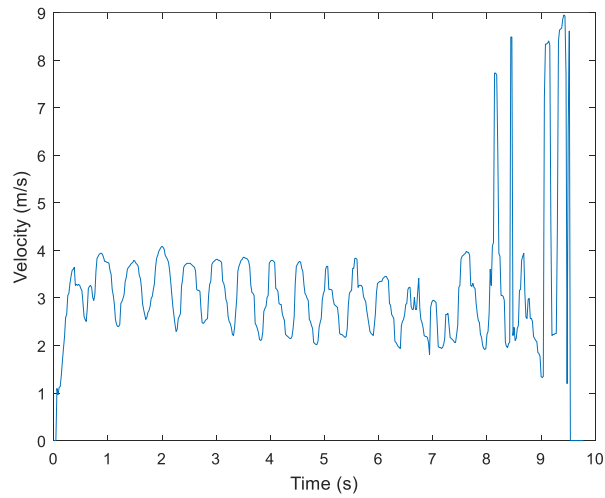


Figure 3.3 Foot Velocity

To curve fit the envelope data and find the expression, the envelope data is smoothed as shown in Figure 3.4. Each effective step's peak velocity is marked by a red dot.

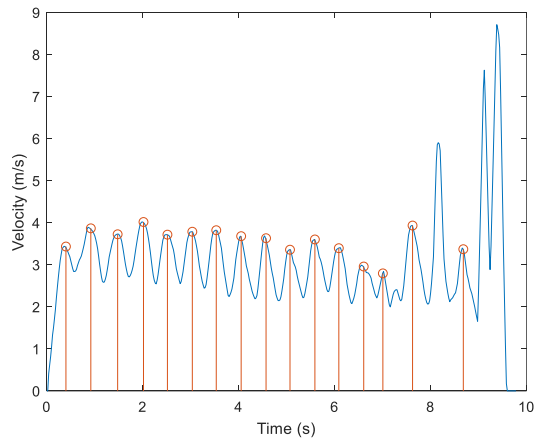


Figure 3.4 Smoothed Data with Peak Foot Velocity

There are steps to find the final expression of the curve. The first step is Gaussian fit curve. A general Gaussian function is as following.

$$f(x) = a_g * e^{-\frac{(x-b_g)^2}{c_g^2}} \quad (3.1)$$

It will become a simple parabola after taking natural logarithm.

$$\ln(f(x)) = \ln(a_g) - \frac{(x-b_g)^2}{c_g^2} \quad (3.2)$$

$$\ln(f(x)) = -\frac{1}{c_g^2}x^2 + \frac{2b_g}{c_g^2}x + (\ln(a_g) - \frac{b_g^2}{c_g^2}) \quad (3.3)$$

or

$$g(x) = ax^2 + bx + c \quad (3.4)$$

Then, fit the velocity in log scale with multiple parabolas that has peak velocities marked. Finally, solve the coefficients for the Gaussian function to get the original expressions for the curve.

$$a_g = e^{(c - \frac{b^2}{4a})} \quad (3.5)$$

$$b_g = -\frac{b}{2a} \quad (3.6)$$

$$c_g = \sqrt{-\frac{1}{a}} \quad (3.7)$$

Where a, b, and c are coefficients for Equation 3.4.

The second step is cosine fit the walking data. The purpose of this step is to eliminate spread out parts near the bottom of Gaussian functions as there is a time that foot velocity approach to zero recognize as Stance Time. A single cosine function is expressed as following.

$$h(x) = a_{cos} \cos(b_{cos}x + c_{cos}) \quad (3.8)$$

where

$$a_{cos} = a_g \quad (3.9)$$

The location of each cosine function is determined by the peak of each wave found in the previous steps. The result is shown in Figure 3.5.

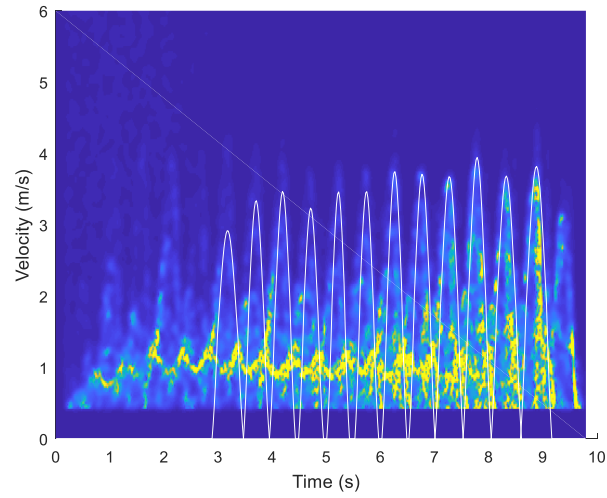


Figure 3.5 Curve Fitted Foot Velocity

3.2 GAIT DATA CALCULATION AND APPROXIMATION

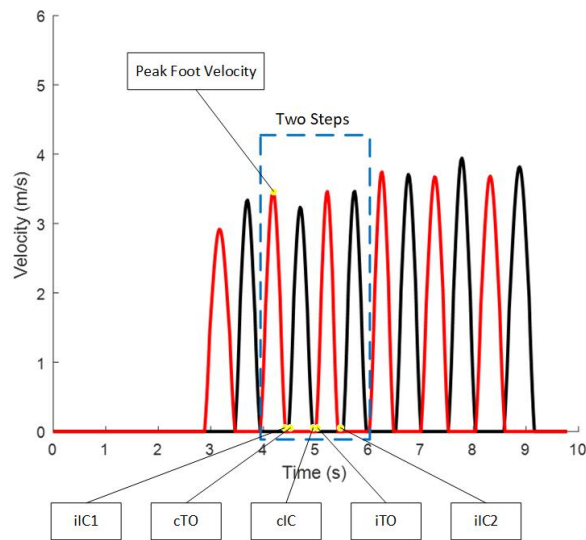


Figure 3.6 Ipsilateral (Red) and Contralateral (Black) Steps

With all the cosine fit functions, different gait parameters can then be derived. Figure 3.6 labels the left foot (defined as ipsilateral) steps and right foot (contralateral) steps with either red or white color. The ipsilateral foot is the foot belonging to or occurring on the same side of the body. Contralateral foot denotes the foot on side of the body opposite to that specified in ipsilateral foot. The following 5 points of each 2 steps marked in Figure 3.6 are used to calculate gait parameters.

- 1) $iIC1$ = first ipsilateral initial foot contact
- 2) cTO = contralateral toe off
- 3) cIC = contralateral initial foot contact
- 4) iTO = ipsilateral toe off
- 5) $iIC2$ = second ipsilateral initial foot contact

3.2.1 Peak Foot Velocity

Peak foot velocity is the maximum forward velocity of the swing foot during a step [19]. It can be observed alternating between two feet. The final number is the average of all steps while the both the average ipsilateral foot peak velocity and average contralateral foot peak velocity are stored respectively for future use.

3.2.2 Stance Time

The stance time is the duration from ipsilateral foot contact to ipsilateral foot off, which is expressed as “ $iTO - iIC1$ ” shown in Figure 3.6. The mean stance time in the gait analyzing procedure represents the average of stance time of both feet.

3.2.3 Swing Time

Swing time is the duration from ipsilateral foot off to ipsilateral foot contact or the time that the foot is in the air. It is expressed as “ $iIC2 - iTO$ ” shown in Figure 3.6. The mean swing time in the gait analyzing procedure represents the average of swing time of both feet.

3.2.4 Stride Time (Gait Cycle)

Stride time, also known as gait cycle, is the duration of two consecutive footsteps from the contact of the ipsilateral foot to the next contact by the ipsilateral foot [20]. A single stride time is expressed as “ $iIC2 - iIC1$ ” shown in Figure 3.6 or simply “stance time

+ swing time”. The mean stride time in the gait analyzing procedure represents the average of stride time of both feet.

3.2.5 Swing/Stance Ratio

As it named, the swing to stance ratio equals the swing time divided by the stance time. The mean swing/stance ratio in the gait analyzing procedure represents the average of each ratio of both feet. A typical swing to stance ratio is 40 : 60 or closer to each other [21]. It serves as good clinical tool to measure success of operation [22].

3.2.6 Stance Time Percentage

Stance Time Percentage (StanceTimePGC) is defined as the percentage of stance time during a full gait cycle, expressed as:

$$StanceTimePGC = \frac{Stance\ Time}{Stride\ Time} \times 100\%$$

The mean stance time percentage in the gait analyzing procedure represents the average of each percentage of both feet.

3.2.7 Step Cadence

The step cadence is defined as number of steps per minute (derived from peak foot velocity measurements). Expressed as:

$$Step\ Cadence = 60 \times \frac{N - 1}{t_{last\ step} - t_{first\ step}}$$

where N is the number of steps observed, $t_{last\ step}$ is time that the last step peak velocity is

observed, and $t_{\text{first step}}$ is time that the first step peak velocity is observed.

3.2.8 Stride Distance (Stride Length)

The stride distance is the distance from the contact of the ipsilateral foot to the next contact by the ipsilateral foot, or the displacement of foot between iIC1 and iIC2 that shown in Figure 3.6. The distance is calculated by integrating the velocity during the time. The mean value of the stride distance is average of each foot stride distances within a walk.

3.2.9 Average Stride Velocity

Average stride velocity, also known as average foot velocity, is defined as the average velocity of a foot during a swing. Notice that the stance time during a stride does not count. Therefore, the expression is as following.

$$\text{Average Stride Velocity} = \frac{\text{Stride Distance}}{\text{Swing Time}}$$

The mean value of average stride velocity is the average of all steps' average stride velocity.

3.2.10 Double Stance Time

Double stance time is the amount of time that both feet are touching the ground, from heel down of one foot to toe off of the other [23]. In healthy normal gait, this happens twice per stride (once for each step), with each representing approximately 15% of the total stride time. An initial double stance time is expressed as “cTO – iIC1”, and a late double stance time is expressed as “iTO - cIC” depending on which foot is defined as the ipsilateral

foot. The mean double stance time is the average of all double stance time during a walk.

3.2.11 Symmetry Index

Symmetry Index a method of percentage assessment of the differences between gait parameters for both lower limbs during walking. SI of 0 is full symmetry. The equation for deriving SI is:

$$SI = \frac{|X_L - X_R|}{0.5(X_L + X_R)} \times 100\%$$

where X_L is the variable recorded for the left leg and the X_R is the variable recorded for the right leg [24]. Variables, such as amplitude of the measurement, average foot velocity, and swing time have been used to calculate the symmetry index in the gait analyzing procedure.

3.2.12 Gait Speed

Gait speed is defined as stride distance (length) divided by stride time. It is considered to be the six vital sign like blood pressure, which may be a general indicator that can predict future events and reflect various underlying physiological processes [25]. The mean value of gait speed in the procedure represents the average gait speed of every strides.

3.2.13 Walk Ratio

Walk ratio is defined as step length/cadence. Using the previous notation it is

expressed as Mean Stride Distance divided by Step Cadence. It is a speed-independent index that reflects energy expenditure, balance, between-step variability, and attentional demand [26].

3.2.14 Results Example

```
meanPeakFootVels: 3.5378
peakFootVelsSTD: 0.2840
meanStanceTimes: 0.5840
stanceTimesSTD: 0.0363
meanSwingTimes: 0.4583
swingTimesSTD: 0.0536
meanStrideTimes: 1.0360
strideTimesSTD: 0.0450
meanSwingStanceRatio: 0.7848
meanStanceTimePGC: 56.4351
stanceTimePGCSTD: 3.8098
stepCadence: 115.3846
meanStrideDistances: 1.0307
strideDistancesSTD: 0.1585
meanAverageStrideVelocities: 2.2458
averageStrideVelocitiesSTD: 0.1809
meanDoubleStanceTimes: 0.0520
Slamp: 0.6078
Slvels: 0.3140
swingTimeSl: 2.1818
meanGaitSpeed: 1.0028
walkRatio (reciprocal): 111.9491
```

Figure 3.7 Sample Result

4. CONCLUSION AND FUTURE DEVELOPMENT

4.1 Conclusion

The presented 4th generation ultrasonic walking gait measurement device has an improved performance, usability, and reliability compared to previous generations. Improper hardware LTI analog to digital conversion board was been replaced by the Measurement Computing 1608 that match the software set up in order to improve the accuracy of the calculation. Further, a separate crystal oscillator, preamplifier, and analog filter in the 3rd generation were integrated onto a single circuit board to reduce the power consumption and data distortion. The previous wide range PIR sensor has been substituted by a spot detection PIR sensor constrained by a Fresnel lens to decrease the redundant data calculation and verification. A gait analyzing procedure has been developed and programmed in C and GNU Octave programming language that run on a Raspberry Pi to achieve on-board calculation. The test result shows that the image processing program runs on a raspberry pi is significantly slower than that on a desktop computer. However, it is acceptable for the 4th generation in-house device, as the calculation can be done at its stand-by time where the live feed is not necessary.

4.2 Future Development

Although the device is currently capable of transmitting data through WIFI and Bluetooth, a fully functional smart phone application or online database has not been established. Such an application or website can be developed in the future, which will dramatically improve the user experience. A neural network is a suitable resource that can train the device to recognize certain walking patterns of different family member when applied in a home. Currently, walking data from different patients need to be manually separated or stated at beginning. A STM32 microcontroller has already been tested in order to substitute the Measurement Computing board as an ADC controller in the future.

BIBLIOGRAPHY

- [1] J. H. Hollman, E. M. McDade and R. C. Petersen, "Normative spatiotemporal gait parameters in older adults," *Gait & Posture*, vol. 34, (1), pp. 111-118, 2011.
- [2] J. Verghese *et al*, "Quantitative gait dysfunction and risk of cognitive decline and dementia," *Journal of Neurology, Neurosurgery, and Psychiatry*, vol. 78, (9), pp. 929-935, 2007.
- [3] M. E. Taylor *et al*, "Gait parameter risk factors for falls under simple and dual task conditions in cognitively impaired older people," *Gait & Posture*, vol. 37, (1), pp. 126-130, 2012;2013;.
- [4] Y. Li *et al*, "A gait analysis system using two cameras with orthogonal view," in 2011, . DOI: 10.1109/ICMT.2011.6002046.
- [5] E. E. Stone and M. Skubic, "Capturing habitual, in-home gait parameter trends using an inexpensive depth camera," in 2012, . DOI: 10.1109/EMBC.2012.6347142.
- [6] R. G. Raj, V. C. Chen and R. Lipps, "Analysis of radar human gait signatures," *IET Signal Processing*, vol. 4, (3), pp. 234, 2010.
- [7] J. Park *et al*, "Simulation and analysis of polarimetric radar signatures of human gaits," *IEEE Transactions on Aerospace and Electronic Systems*, vol. 50, (3), pp. 2164-2175, 2014.
- [8] Z. Xue *et al*, "Infrared gait recognition based on wavelet transform and support vector machine," *Pattern Recognition*, vol. 43, (8), pp. 2904-2910, 2010.
- [9] R. Ricci *et al*, "Classification of gait patterns through an ultrasound-doppler motion

- analysis system," *Gait & Posture*, vol. 42, pp. S22-S23, 2015.
- [10] A. Matić et al, "Infrared assessment of knee instability in ACL deficient patients," *International Orthopaedics*, vol. 40, (2), pp. 385-391, 2016.
- [11] R. K. Begg *et al*, "Real-time biofeedback of gait parameters using infrared position sensors," in 2012, . DOI: 10.1109/ICSensT.2012.6461777.
- [12] J. Sabatier and A. Ekimov, "Rhythm analysis of orthogonal signals from human walking," *The Journal of the Acoustical Society of America*, vol. 129, (3), pp. 1306-1314, 2011.
- [13] D. Komma, "Ultrasonic Doppler Sonar Sensor System for Extraction of Walking Signature", Undergraduate, University of Mississippi, 2016.
- [14] F. Gamble, "Multidimensional Motion Capture Using Doppler Ultrasonic", Undergraduate, University of Mississippi, 2016.
- [15] M. Bradley *et al*, "Extraction of the velocity of walking human's body segments using ultrasonic Doppler," *The Journal of the Acoustical Society of America*, vol. 128, (5), pp. EL316-EL322, 2010.
- [16] A. Mehmood, J. M. Sabatier, and T. Damarla, "Ultrasonic Doppler methods to extract signatures of a walking human," *The Journal of the Acoustical Society of America*, vol. 132, no. 3, pp. 243–249, Aug. 2012.
- [17] R. Lyons, "A Quadrature Signals Tutorial: Complex, But Not Complicated," *DSPRelated.com / DSP*, 12-Apr-2013. [Online]. Available: <https://www.dsprelated.com/showarticle/192.php>. [Accessed: 25-Feb-2018].

- [18] “Wiener filter,” *Wikipedia*, 17-Feb-2018. [Online]. Available: https://en.wikipedia.org/wiki/Wiener_filter. [Accessed: 25-Feb-2018].
- [19] A. R. De Asha and J. G. Buckley, "The effects of walking speed on minimum toe clearance and on the temporal relationship between minimum clearance and peak swing-foot velocity in unilateral trans-tibial amputees," *Prosthetics and Orthotics International*, vol. 39, (2), pp. 120, 2015.
- [20] O. Beauchet *et al*, "Walking speed-related changes in stride time variability: effects of decreased speed," *Journal of Neuroengineering and Rehabilitation*, vol. 6, (1), pp. 32-32, 2009.
- [21] M. Iosa *et al*, "The Golden Ratio of Gait Harmony: Repetitive Proportions of Repetitive Gait Phases," *BioMed Research International*, vol. 2013, pp. 1-7, 2013.
- [22] M. Loke, “Swing Phase Control and Stance Phase Control,” *Swing Phase Control - Stance Phase Control - DBS™*. [Online]. Available: http://www.dynamicbracingsolutions.net/Pages/Bracing_Concepts/Swing_Stance_Control.html. [Accessed: 24-Mar-2018].
- [23] S. R. Goldberg *et al*, "Muscles that influence knee flexion velocity in double support: implications for stiff-knee gait," *Journal of Biomechanics*, vol. 37, (8), pp. 1189-1196, 2004.
- [24] S. Nigg *et al*, "Development of a symmetry index using discrete variables," *Gait & Posture*, vol. 38, (1), pp. 115-119, 2012;2013;.
- [25] S. Fritz and M. Lusardi, "White Paper: "Walking Speed: the Sixth Vital

Sign", *Journal of Geriatric Physical Therapy*, vol. 32, (2), pp. 2, 2009.

- [26] V. Rota *et al*, "Walk ratio (step length/cadence) as a summary index of neuromotor control of gait: application to multiple sclerosis," *International Journal of Rehabilitation Research*, vol. 34, (3), pp. 265-269, 2011.